Appearing in May 2006 PASP

Variable Unidentified Emission Near 6307 Å in η Carinae[1,2]

J. C. Martin[3]

K. Davidson[3]

F. Hamann[4]

O. Stahl[5]

K. Weis[6,7]

ABSTRACT

We have discovered a conspicuous unidentified variable feature near 6307 Å in the spectrum of η Carinae which is spatially unresolved from the central star and its wind ($r \lesssim$ 200–300 AU). It is significant for two reasons: such prominent unidentified lines are now rare in this object, and this feature varies strongly and systematically. It exhibits a combination of characteristics which, so far as we know are unique in η Carinae's spectrum. It may provide insights into the recurrent spectroscopic events and the star's long-term brightening.

Subject headings: binaries: general, line: profiles, stars: individual (η Carinae), stars: variables: other, stars: winds, outflows

---

[1]This research is part of the Hubble Space Telescope Treasury Project for Eta Carinae, supported by grants GO-9420 and GO-9973 from the Space Telescope Science Institute (STScI), which is operated by the Association of Universities for Research in Astronomy, Inc., under NASA contract NAS 5-26555.

[2]Partially based on observations obtained with UVES at the ESO Very Large Telescope, Paranal, Chile (proposals 70.D-0607(a), 71.D-0168(A), and 072.D-0524(A))

[3]School of Physics and Astronomy, University of Minnesota, 116 Church Street SE, Minneapolis, MN 55455; martin@etacar.umn.edu

[4]Department of Astronomy, University of Florida, P.O. Box 112055, Gainesville, FL 32611

[5]Landessternwarte Heidelberg, Königsstuhl, 69117 Heidelberg, Germany.

[6]Astronomisches Institut, Ruhr-Universität Bochum, Universitätsstrasse 150, D-44780 Bochum, Germany

[7]Lise Meitner Fellow

1. Introduction

The spectrum of η Carinae has been extensively studied and characterized, but unexpected changes can happen during a spectroscopic event like the one that occurred in mid-2003. For instance, surprisingly strong high-excitation He II λ4687 briefly appeared at that time as reported by Steiner & Damineli (2004), Stahl et al. (2005) and Martin et al. (2006); see the last of those papers for an analysis of its significance. Motivated by this example, we have examined Hubble Space Telescope (HST) data for other transient features. Our search yielded an undiagnosed emission feature at 6307 Å with good signal-to-noise and unusual behavior.

These data were obtained with the Space Telescope Imaging Spectrograph (STIS), whose high spatial resolution allowed us to examine the central star itself (or rather its inner wind) separate from the bright nearby ejecta that contaminate all ground-based spectroscopy of η Car (Figure 1).

The 6307 Å feature is spatially unresolved from the continuum emission of the central star and its wind in the STIS CCD data. It does not match any of the known atomic or molecular transitions of any species that we expect to find in the spectrum (see Thackeray (1953), Zethson (2001a) (Table 1), and Wallerstein et al. (2001) for extensive lists of species identified in η Car). This is a significant discovery because, unlike the few other noticeable lines that have not yet been identified, the 6307 Å emission varies conspicuously. It is obviously correlated with η Car's 5.5-year spectroscopic period; indeed it temporarily disappeared during the 1998 and 2003 spectroscopic events. Moreover, following the 2003 event this feature became much stronger than it had been in the previous cycle, possibly indicating a link with the rapid brightening and other mysterious developments that have been superimposed on the 5.5-year cycle since the mid-1990's (Davidson et al. 1999; Martin & Koppelman 2004; Davidson et al. 2005). Altogether, it is unique in the small set of lines which remain unidentified in η Car's spectrum.

2. The Data

2.1. Spectra

The HST/STIS spectra in this paper were obtained as part of the η Carinae HST Treasury Project (Davidson 2004) and were reduced using a modified version of the Goddard CALSTIS reduction pipeline (Table 2). The modified pipeline uses the normal HST bias subtraction, flat fielding, and cosmic ray rejection procedures with the addition of improved

pixel interpolation and improved bad/hot pixel removal. Information regarding these modifications can be found online at our web site[1] and in a forthcoming publication (Davidson et al., *in preparation*). The spectra are reduced and extracted using approximately the same parameters used by Martin et al. (2006). Each one-dimensional STIS spectrum discussed here is essentially a 0.1″ x 0.25″ spatial sample: the pixel size is about 0.05″, the slit width is about 2 CCD columns, each spectral extraction sampled 5 CCD rows, and the spectral resolution is roughly 52 km s^{-1} at 6307Å. We applied an aperture (extraction height) correction to the absolute flux, based on an observation of the spectrophotometric standard BD +75 325 with the same slit and extraction parameters. Such details have little effect on the main results of this paper.

In addition to the HST/STIS spectra, we used spectra of the central star observed with the ESO VLT/UVES. That observing program is described in detail by Weis et al. (2005a) and Weis et al. (2005b). Each one-dimensional UVES spectrum is a 0.30″ x 0.91″ spatial sample: the pixel size is about 0.182″, the slit width is just under 2 CCD columns, each spectral extraction sampled 5 CCD rows, the seeing ranged from 0.5″ to 1.3″, and the spectral resolution is roughly 3.75 km s^{-1} at 6307Å. We corrected the wavelength scale to the heliocentric reference frame using the IRAF procedure noao.rvcorrect. These spectra are not absolute flux calibrated.

In ground-based spectra, like those from the VLT/UVES, strong atmospheric absorption bands and emission lines from the bright ejecta make it difficult at some wavelengths to detect even dramatic changes in the spectrum of the central star. In the VLT/UVES spectra, sharp lined atmospheric O_2 absorption is observed around 6307Å and sharp nebular Fe II λ6307.04 and Cr II λ6307.39 formed in the nearby ejecta are blended with the stellar spectra. The HST/STIS are unlike ground-based observations in that they are free of atmospheric absorption and specifically include only the region within $r \approx$ 200–300 AU of the central star. Here "the star" or "η Carinae," means the central object and its wind, excluding the bright ejecta and Homunculus nebula (Figure 1). If the star is double then it is unresolved by the HST.

2.2. Photometry

Figure 5 uses HST ACS/HRC data obtained as part of the HST treasury project. These data are summarized in Table 3 of Martin & Koppelman (2004). The bias-corrected, dark-subtracted, and flat-fielded images were obtained from the Space Telescope Science Institute

[1] `http://etacar.umn.edu`

via the Multi-Mission Archive (MAST) (Sirianni et al. 2005)[2] and measured with a 0.3″ radius ($\sim$ 10 ACS/HRC pixels) weighted aperture described by Martin & Koppelman (2004). The measured flux is corrected to an infinite aperture using factors we derived following Sirianni et al. (2005) from archived observations of the star GD71. The corrected fluxes were converted to the STMAG system (Sirianni et al. 2005) using the standard photometry keywords provided by the STScI reduction pipeline in the FITS headers.

The ACS/HRC data are supplemented by photometry synthesized from flux calibrated STIS CCD spectra. A summary of the spectra are given in Table 2. They were extracted with a cross dispersion weighting function which matched the 0.3″ aperture used to measure the ACS/HRC images. We applied an aperture (extraction height) correction based on an observation of the spectrophotometric standard star BD +75 325 with the same slit and extraction techniques. The spectra were convolved with the published ACS/HRC filter and CCD response functions and then integrated to obtain synthetic fluxes. Finally, the synthetic fluxes were adjusted to the STMAG system by comparing the synthetic results to results from ACS/HRC observations on the same day (MJD 52682).

3. Overview of the Feature

The unidentified emission feature appeared in the wing of the Fe II λ6319 line near 6307Å (Figure 2, Figure 3 and Table 3). It had a FWHM of about 150 – 180 km s^{-1} which is narrower than the stellar wind features (FWHM $\approx$ 300 - 500 km s^{-1}) but significantly broader than the nebular emission from the surrounding bright ejecta (FWHM $\approx$ 10 km s^{-1} (Zethson 2001a)[3]).

The feature is also present in the spectrum of the star reflected by the Homunculus lobes (see the VLT/UVES FOS4 slit setting described by Weis et al. (2005a)). The equivalent width of the feature is smaller there. However there is no variation of its profile along the UVES slit except for the radial velocity shift introduced by motion of the reflecting ejecta. This leads us to conclude that, unlike Hα (Smith et al. 2003), there is no obvious variation of this feature with stellar latitude.

---

[2] `http://archive.stsci.edu`

[3] The spectral resolution of the STIS was roughly 52 km s^{-1} at 6307Å. Therefore, the spectral width of the nebular emission lines is not resolved in the STIS/CCD data.

4. Identification

We have been unable to find any known transitions consistent with other lines present in the spectrum that match this feature. We ruled out S II λ6307 because none of the associated transitions with similar levels and oscillator strengths at 6314.4Å, 6288.6Å, or 6288.0Å appeared in the spectrum. Another possible identification may be [O I] λ6302.0 redshifted by 100 – 200 km s^{-1}. Nearly all the atomic oxygen in the wind of the central star is probably ionized. O I λ1302, λ1307, and λ1306 are present in the HST/MAMA data but they are *blueshifted* by 400 to 500 km/s. However, the [O I] λ6365 is not present and a 100 km s^{-1} redshift would be anomalous. Therefore, the 6307Å emission is probably not [O I] λ6302.0. Thackeray (1953), Damineli et al. (1998), Wallerstein et al. (2001), and Zethson (2001a) reported [O I] λ6302.0 in their spectra, but the line they describe is narrow, redshifted, and originates in the surrounding bright ejecta, not the central star (Figure 1). Its wavelength obviously differs from the feature that we discuss.

We considered emission pumped by Lyman α, Since η Car is a significant source of Lyman α emission, and resonance with that emission plays a role in the formation of other features (Martin et al. 2006; Johansson & Hamman 1994; Zethson et al. 2001b). We found three transitions between 6305 Å – 6309 Å that are resonant with absorption features within 3 Å of Lyman α: Cr II λ6305.75 (resonant with λ1213.499), Cr III] λ6306.8 (resonant with λ1215.781), and Fe III] λ6306.43 (resonant with λ1213.41). The oscillator strengths have not been measured for any of these transitions. While all these species appear in the nebular spectra of the nearby ejecta, they are not found in the stellar spectrum. Furthermore, we do not see these specific transitions in the nebular spectra along with other previously identified resonance type features. Altogether it is difficult to judge the likelihood of these possible identifications. However, there is some appeal to identifying it as an ionized metal line, since aspects of its variability are similar to those exhibited by the broad components of the Fe II lines and the metal absorption forest around 2500Å (see next section).

There is an emission line in the spectrum of the surrounding ejecta and Weigelt Knots at 6306.3 Å which Zethson (2001a) identified as Fe II λ6307.04 and Cr II λ6307.39 (Table 1). That line in the spectrum of the ejecta has a much sharper profile (FWHM $\approx$ 10 km s^{-1}) than 6307Å in the spectrum of the star. Fe II λ6307.0 and Cr II λ6307.4 are also clearly formed in the area of extended emission within half an arc second of the star that is resolved by the HST/STIS. They are not found in the spectrum of the star itself, whereas the region emitting 6307Å is spatially unresolved from the central star (Figure 1).

5. Variability of the Feature

The 6307Å feature *disappeared* during the 1998.0 and 2003.5 spectroscopic events (Figure 4) at the same time when the Hydrogen Balmer absorption strengthened and broad high excitation emission (such as He I) weakened. It gradually declined in flux over the six months prior to the 2003.5 event but just before disappearing completely its decline was interrupted by a brief upward tick in brightness lasting a few weeks (Figure 5). The only other component of the spectrum exhibiting similar behavior just preceding the event is the "iron curtain" of blanketed near-ultraviolet (NUV) absorption. One plausible explanation for this brief "hiccup" is a sudden change in ionization caused by a increase in the ionizing flux from the central star. In that case, 6307Å is a metal line whose population is markedly increased as the species in the "iron curtain" are further ionized and temporarily depleted.

The 6307 Å feature also evolved much more than most other lines between the spectroscopic events. A similar degree of activity is observed in the broad components of the Fe II lines formed in the central star's wind (Figure 6). Note that around 2001 (at a time between spectroscopic events), 6307 Å is anti-correlated with Fe II emission. Like the NUV flux, a rise in 6307 Å brightness was anti-correlated with Fe II emission.

The aspects of variability which 6307 Å shares with Fe II indicate that it is probably also an ionized metal line formed in the stellar wind. The most viable candidates are the transitions we noted as being in resonance with Lyman α (Cr II λ6305.75, Cr III] λ6306.8, and Fe III] λ6306.43). For obvious reasons, Fe III] λ6306.43 is the most enticing option. Unfortunately, the atomic data for that transition is lacking so that we are unable to confirm our suspicions.

6. Mid-Cycle Phenomena: Evidence for Extra-Cyclical Processes?

In most proposed explanations of the 5.5-year spectroscopic period *there is no obvious reason to expect much variability in mid-cycle*, e.g., during 1999–2001 halfway between the 1998.0 and 2003.5 spectroscopic events. In the most popular scenario describing these events, the cycle is regulated by a companion star in a highly eccentric orbit as sketched in Figure 7. At distances of 20–30 AU from the primary star, where the hypothetical companion should have been during 1999–2001, relevant wind densities are factors of 30 to 100 smaller than at periastron. Column densities are correspondingly small and the motion is quite slow. Therefore we do not expect orbital motion alone to precipitate appreciable spectroscopic changes during that part of the cycle. Analogous comments can be made if the 5.5-year period is a single-star thermal/rotational recovery cycle between outbursts, although such

models are admittedly less definite. For these reasons, any rapid or pronounced changes observed in 1999–2001 were most likely *not* due to the 5.5-year cycle; instead they probably give us information about LBV-like random fluctuations in the stellar wind. If this statement is wrong, then the mid-cycle variations reveal an aspect of the cycle that has no explanation in any proposed models. In either case it is important to study the features that did vary then. Among them the unidentified 6307 Å varied most strongly.

In our HST/STIS data during the 1998–2003 cycle this line was brightest in 2001.29 (MJD 52016.8). Our temporal sampling was too sparse to indicate the true peak, but on that occasion the line was more than twice as strong as it had been in 1999-2000 (Figure 4).

Meanwhile, several other changes occurred in 2001, about the same time as the maximum 6307 Å strength:

- A 0.05 magnitude dip in J, H, and K brightness (Whitelock et al. 2004),
- A roughly 20% increase in near-ultraviolet flux around 1800Å over the course of nine months,
- A 15%–20% fluctuation in flux emitted in the broad components of the Fe II lines formed in the stellar wind over the course of nine to twelve months (see Fig. 6),
- An 20%–30% decrease in Hydrogen Balmer P-Cygni absorption (Davidson et al. 2005),
- A 10%–20% increase in the total Hydrogen Balmer emission flux (Davidson et al. 2005),
- A sudden and significant increase in the strength of the narrow -140 km s^{-1} absorption feature in the Hydrogen Balmer lines.

While these events were simultaneous, we have no proof that they are physically related. There is no clear reason or explanation why any feature should undergo significant change in the *middle* of the spectroscopic cycle. As noted, in almost any binary star model of the 5.5-year cycle, the two components were far apart and moving slowly in 2001. The moderate changes listed above may perhaps be ascribed to ordinary LBV-like fluctuations. Although taken all together at the same time they are suggestive of some other process at work in addition to the spectroscopic cycle. This aspect of the overall problem of mid-cycle behavior has received little attention to date.

After the maximum, the emission feature slowly faded over the next two years until it disappeared completely in the lead up to the 2003.5 event. After the event, the feature recovered. However on MJD 53413 and MJD 53448 the flux of the feature was more than

twice the flux it had at the same phase a cycle earlier (approximately MJD 51500). The fact that the behavior of the feature appears to be different from cycle to cycle suggests that it is affected by some additional parameter, i.e. the long-term brightening trend of the central star.

7. Summary

We have discovered a previously unidentified emission feature in the spectrum of η Carinae: a single emission line at 6307Å. This feature is important because:

- The visual light spectrum of η Carinae has been extensively studied and only about 3% of the features remain unidentified (Zethson 2001a).
- This feature's variability appears to be associated with the variability of Fe II in the wind of the central star.
- It evolves in a unique way with time and thus may provide clues to the nature of the spectroscopic cycle and/or long-term brightening trend.
- The peak in the flux of the feature coincided with several other mid-spectroscopic cycle changes in the spectrum that we cannot explain.
- The 6307Å feature is associated with the spectroscopic cycle, but its behavior does not reproduce exactly from one cycle to the next.

This feature is visible in some spectra of the central star and its wind, but not others during the last seven years. We are unable to match it to any published atomic or molecular transitions of species which we expect to find in the spectrum based on other lines present. Its unidentified and transient nature make it fairly unique in the spectrum of η Carinae. Its disappearance and reappearance correlated with the spectroscopic events, implying that it is associated with the spectroscopic cycle. Its mid-cycle peak and cycle-to-cycle changes are also sufficiently different from other identified features so that it deserves special attention.

The 6307Å feature is visible in ground-based spectra despite being blended with atmospheric O_2 absorption and emission from the surrounding ejecta. We encourage our colleagues in the southern hemisphere to look for it since it varies between spectroscopic events and tracking these variations with better temporal sampling may help provide further insight into the 5.5-year cycle or the recent dramatic brightening of the central star.

8. Acknowledgments

This work made use of the NIST Atomic Spectra Database[4] and the Kentucky Atomic Line List v2.04[5]. We also wish to thank M. Salvo (ANU) for generously using some of her time on the MSO 2.3m to obtain current ground-based spectra for us. T.R. Gull (NASA/GSFC) prepared most of the detailed STIS observing plans, gave other valuable help in the Treasury Program. Meanwhile, K. Ishibashi (MIT) produced the improved reduction software and contributed to the observing plans. We also thank S Johansson, H Hartman (University of Lund), and M. Bautista (Inst. Venezolano Invest. Cientifica) for comments on an early version of this paper, and Beth Periello (STScI) for assistance with the HST observing plan.

[4]http://physics.nist.gov/PhysRefData/ASD/index.html

[5]http://www.pa.uky.edu/∼peter/atomic/index.html

REFERENCES

Damineli, A., Stahl, O., Kaufer, A., Wolf, B., Quast, G., & Lopes, D. F. 1998, A&AS, 133, 299

Damineli, A., Viotti, R., Stahl, A. K. O., Wolf, B., & de Araújo, F. X. 1999, ASP Conf. Ser. 179: Eta Carinae at The Millennium, 196

Davidson, K., Ebbets, D., Weigelt, G., Humphreys, R. M., Hajian, A. R., Walborn, N. R., & Rosa, M. 1995, AJ, 109, 1784

Davidson, K. & Humphreys, R. M. 1997, ARA&A, 35, 1

Davidson, K. et al. 1999, AJ, 118, 1777

Davidson, K., Ishibashi, K., Gull, T. R., Humphreys, R. M., & Smith, N. 2000, ApJ, 530, L107

Davidson, K. 2002, ASP Conf. Ser. 262: The High Energy Universe at Sharp Focus: Chandra Science, 267

Davidson, K. 2004, STScI Newsletter, Spring 2004, 1, http://sco.stsci.edu/newsletter/PDF/2004/spring_04.pdf

Davidson, K. et al. 2005, AJ, 129, 900

Davis, M., Campbell, D., Sticka, R., Faful, B. Leidecker, H., Kimbel, R., & Goudfrooij, P. 2001, STIS Failure Review Board Final Report (Baltimore: STSci)

Hamann, F. & Persson, S. E. 1989, ApJS, 71, 931

Hamann, F., Depoy, D. L., Johansson, S., & Elias, J. 1994, ApJ, 422, 626

Hofmann, K.-H., & Weigelt, G. 1988, A&A, 203, L21

Ishibashi, K. 2001, ASP Conf. Ser. 242: Eta Carinae and Other Mysterious Stars: The Hidden Opportunities of Emission Spectroscopy, 53

Johansson, S. & Hamman, F. W. 1994, Phys. Scr., T47, 157

Martin, J. C., & Koppelman, M. D. 2004, AJ, 127, 2352

Martin, J. C., et al. 2006, ApJ, in press March 2006

Proffitt, C. R. et al. 2002, The 2002 HST Calibration Workshop : Hubble after the Installation of the ACS and the NICMOS Cooling System, Proceedings of a Workshop held at the Space Telescope Science Institute, Baltimore, Maryland, October 17 and 18, 2002. Edited by Santiago Arribas, Anton Koekemoer, and Brad Whitmore. Baltimore, MD: Space Telescope Science Institute, 2002., p.97, 97

Sirianni, M., et al. 2005, PASP, 117, 1049

Smith, N., Davidson, K., Gull, T. R., Ishibashi, K., & Hillier, D. J. 2003, ApJ, 586, 432

Stahl, O., Weis, K., Bomans, D. J., Davidson, K., Gull, T. R., & Humphreys, R. M. 2005, A&A, 435, 303

Steiner, J. E., & Damineli, A. 2004, ApJ, 612, L133

Thackeray, A. D. 1953, MNRAS, 113, 211

Wallerstein, G., Gilroy, K. K., Zethson, T., Johansson, S., & Hamann, F. 2001, PASP, 113, 1210

Whitelock, P. A., Feast, M. W., Marang, F., & Breedt, E. 2004, MNRAS, 352, 447

Weis, K., Stahl, O., Bomans, D. J., Davidson, K., Gull, T. R., & Humphreys, R. M. 2005a, AJ, 129, 1694

Weis, K., Bomans, D. J., Stahl, O., Davidson, K., Humphreys, R. M., & Gull, T. R. 2005b, ASP Conf. Ser. 332: The Fate of the Most Massive Stars, 332, 162

Zanella, R., Wolf, B., & Stahl, O. 1984, A&A, 137, 79

Zethson, T. 2001a, Ph.D. Thesis, Lunds Universitet

Zethson, T., Hartman, H., Johansson, S., Gull, T., Ishibashi, K., & Davidson, K. 2001b, ASP Conf. Ser. 242: Eta Carinae and Other Mysterious Stars: The Hidden Opportunities of Emission Spectroscopy, 242, 97

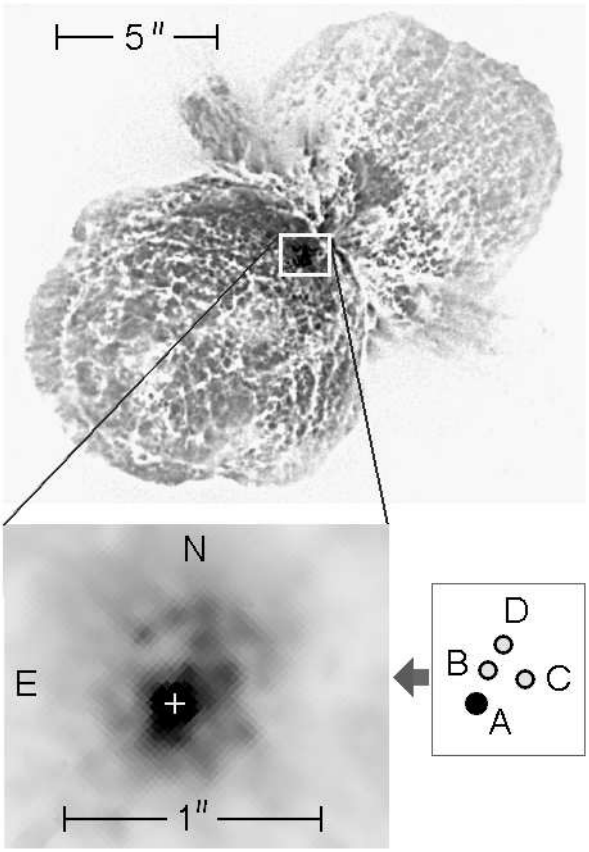

Fig. 1.— Spatial distribution of ejecta mentioned in text. Top: A map of the Homunculus based on HST/WFPC2 images. The small rectangle is the region shown at the bottom. Lower left: HST/ACS image of the inner region, using filter F330W (near UV) in 2005. Lower right: Relative locations of the slow-moving "Weigelt blobs" BCD specified by Hofmann & Weigelt (1988), expanded by 20% to allow for motions. The spatial scale throughout this figure is adjusted to epoch 2005.

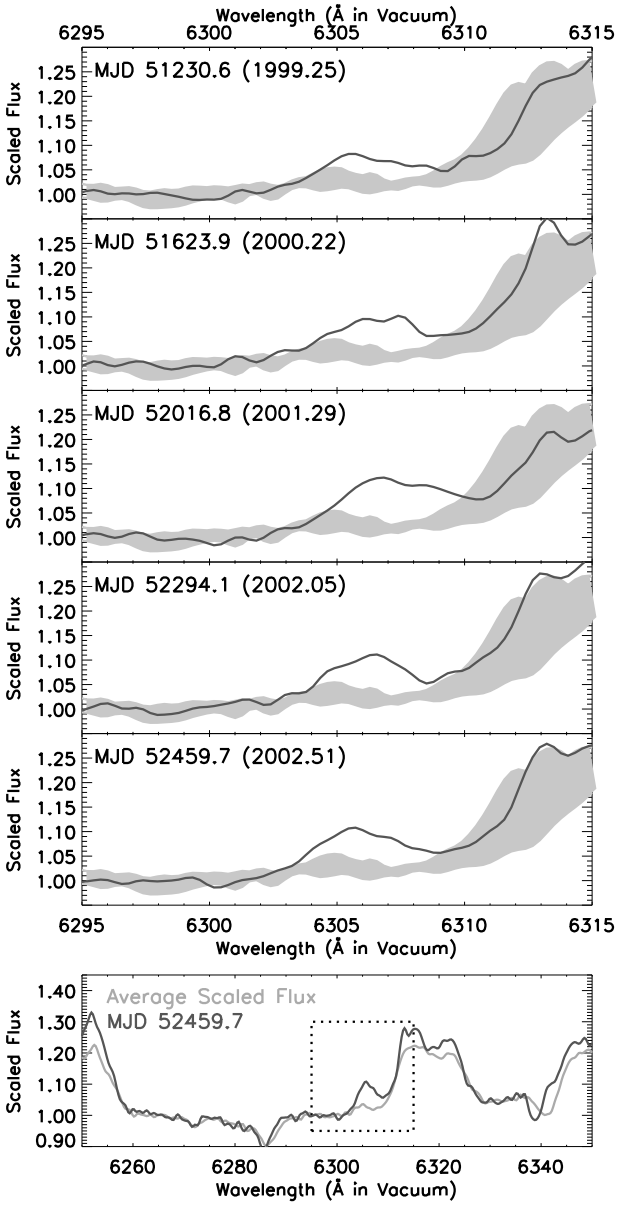

Fig. 2.— Plots of the HST/STIS spectra. Top five panels: Plots of the 6307Å emission on the dates that it was unambiguously present. The gray region in each plot gives the range of relative flux values when the emission was definitely not present during the 2003.5 spectroscopic event. Bottom panel: A plot of the average scaled flux and the flux recorded on MJD 52459.7 over an expanded wavelength range. The dotted box marks the area plotted in the previous panels.

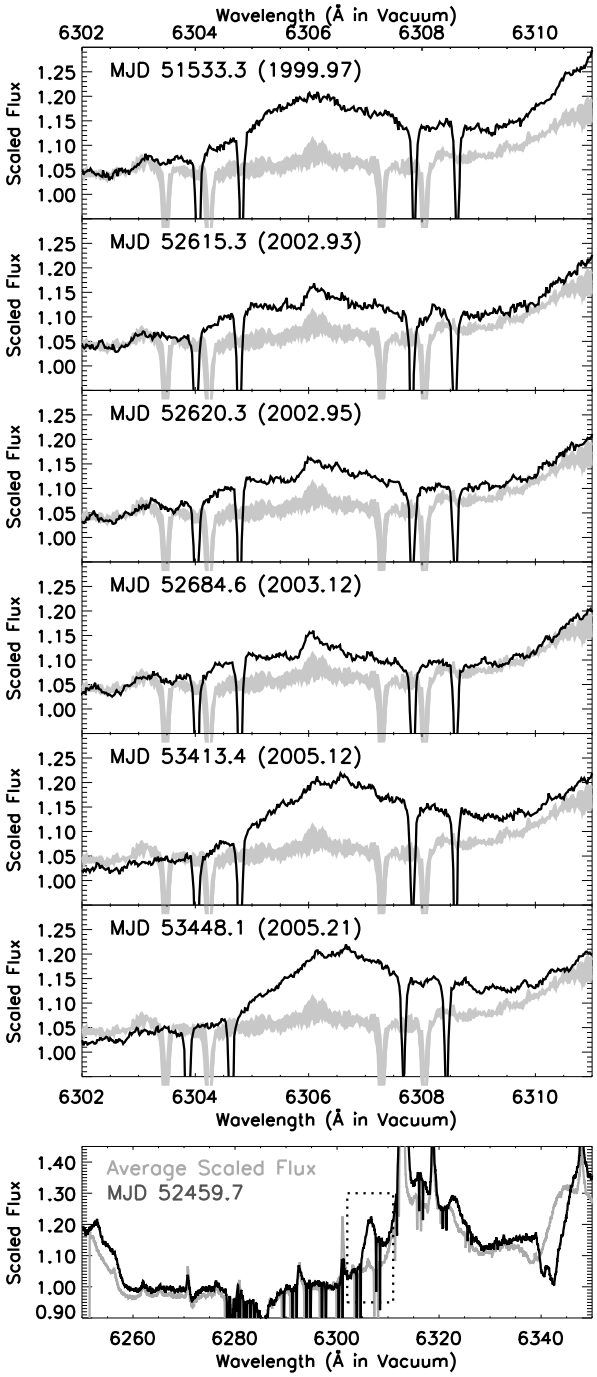

Fig. 3.— Same as for Fig 2 except for the VLT/UVES spectra.

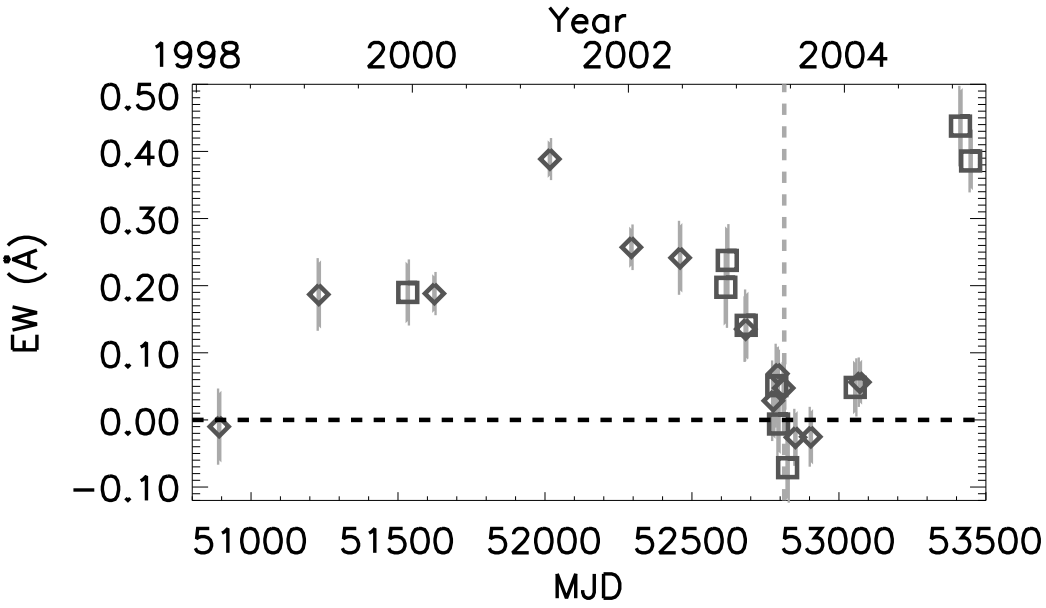

Fig. 4.— The equivalent width of 6307Å emission in the HST/STIS data (diamonds) and VLT/UVES (boxes) in the spectrum of the central star versus time. The vertical ticks on each point are 1σ error bars given in Table 3. The dotted vertical line marks the time of the 2003.5 spectroscopic event.

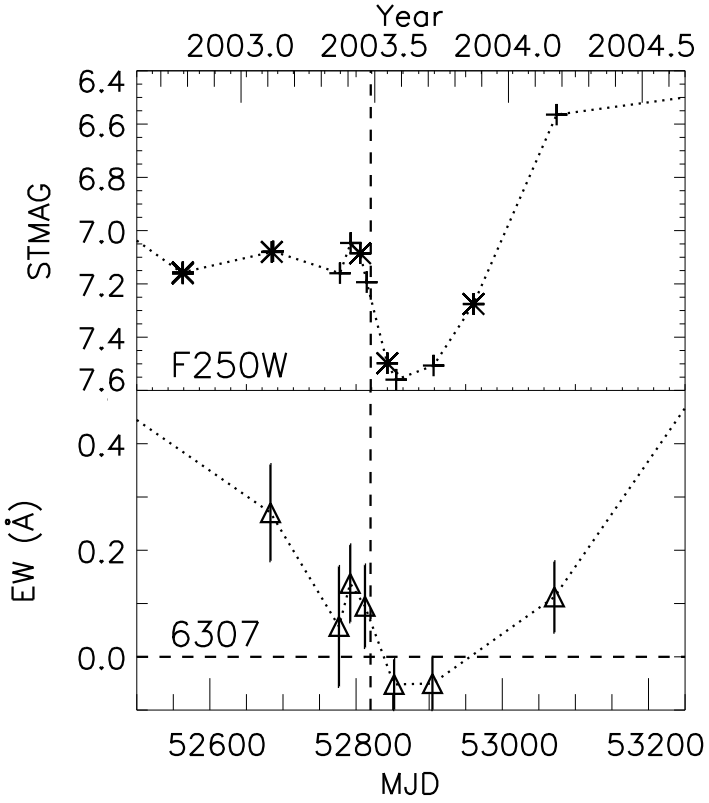

Fig. 5.— Top: NUV in the F250W filter measured with the ACS/HRC (diamonds) and synthesized from flux calibrated STIS/CCD spectra (crosses). The statistical 1σ error of each data point is 0.01–0.02 mag (smaller than the size of the symbols) Bottom: Equivalent width of 6307 Å measured in the STIS/CCD spectra with 1σ error bars estimated from the S/N of the continuum. The vertical dashed line marks the time of the disappearance of the He I line on MJD 52819.8 during the 2003.5 event.

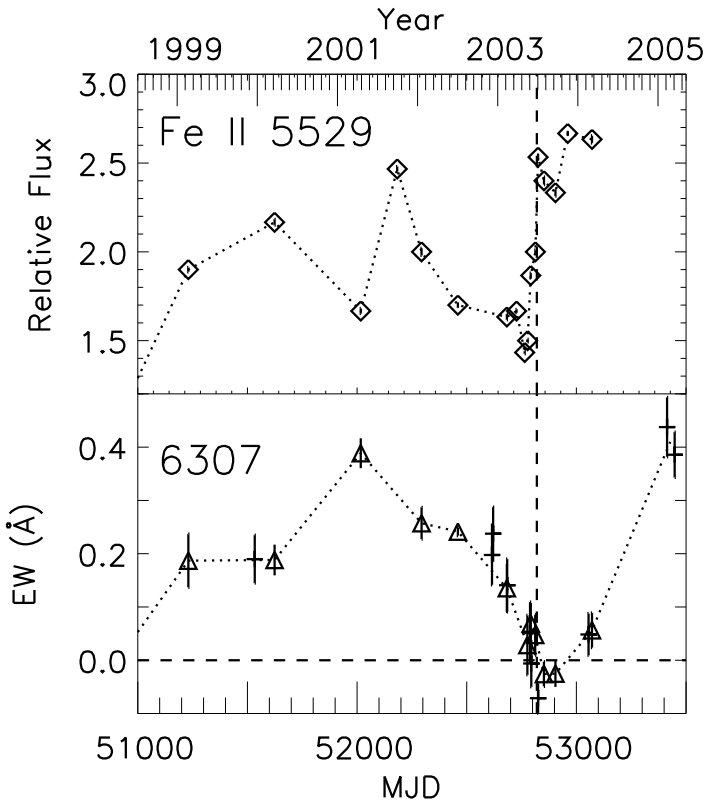

Fig. 6.— Top: Fe II 5529 flux (continuum subtracted) measured in STIS/CCD spectra. The 1σ error in these data are about the size of the plotted symbols. Bottom: Equivalent width of 6307 Å measured in STIS/CCD spectra (triangles) and VLT/UVES spectra (crosses) with 1σ error bars. The vertical dashed line marks the time of the 2003.5 event.

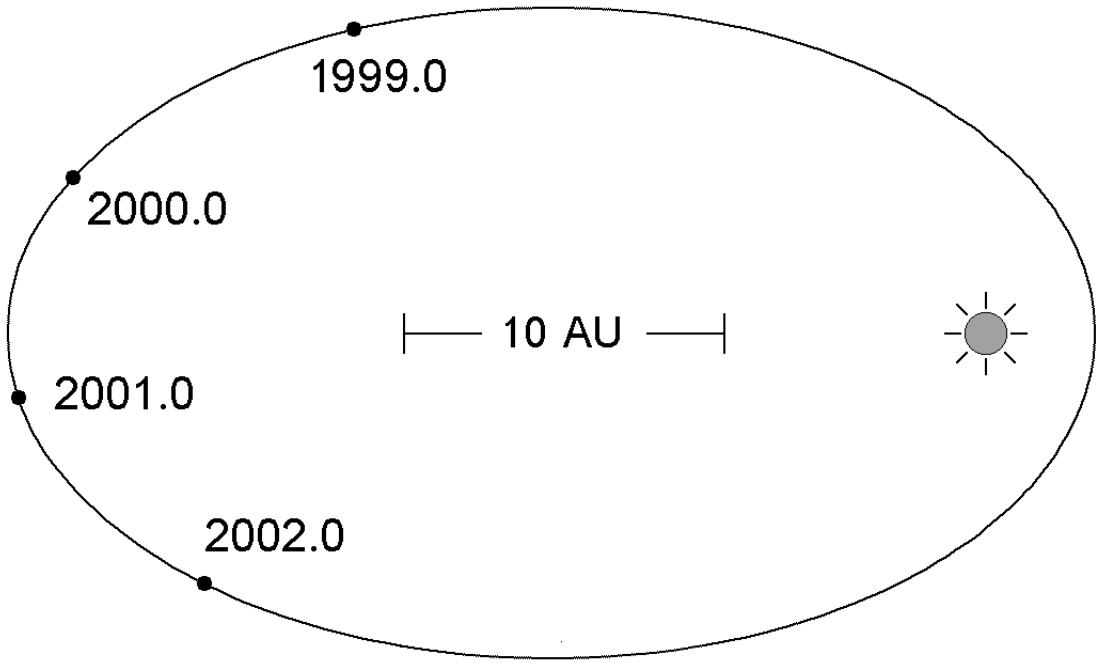

Fig. 7.— Between 1999.0 and 2002.0 the when the 6306 Å feature was still varying the secondary was well separated from the primary. The time of periasteron is uncertain by several weeks but has little effect on this sketch.

Table 1. Narrow Nebular Emission Lines Identified By Zethson Near 6307Å[a]

λ_{obs} Å	Species	Transition	λ_{lab}	Notes[b]
6256.56	Fe II(34)	$b^4F_{3/2} - z^6D_{3/2}$	6257.08	···
6261.88	[Fe II](44F)	$a^2G_{9/2} - b^2F_{5/2}$	6265.93	···
6265.17	[V II]	$a^3D_1 - b^1F_3$	6265.93	id?
···	[V II]	$b^3G_3 - d^3P_1$	6266.33	id?
···	[V II]	$a^3G_5 - d^3F_4$	6266.34	id?
6270.62	Fe II	$b^2H_{11/2} - z^6P_{3/2}$	6271.70	···
6276.44	[Fe II](15F)	$a^4F_{7/2} - a^2P_{3/2}$	6277.2	···
6280.81	[Fe II]	$a^2D2_{3/2} - a^2S_{1/2}$	6281.69	···
···	Fe II]	$b^4F_{5/2} - z^6D_{5/2}$	6281.56	···
6287.00	[Mn II]	$a^5D_2 - a^3P_1$	6287.77	···
6292.65	Fe II	$(^5D)4d^4P_{3/2} - (^5D_0)4f^2[3]_{5/2}$	6293.57	?E_u
6297.32	Unidentified	···	···	···
6301.14	[O I](1F)	$2p^4\ ^3P_2 - 2p^4\ ^1D_2$	6302.05	···
6306.3	Fe II(200)	$c^4F_{9/2} - x^4F_{9/2}$	6307.47	···
···	Cr II	$b^2P_{3/2} - y^2P_{3/2}$	6307.39	···
6308.51	Fe II(34)	$b^4F_{7/2} - z^6D_{7/2}$	6309.27	···
6312.82	[S III](3F)	$3p^2\ ^1D_2 - 3p^2\ ^1S_0$	6313.81	Not in 98
6318.77	Fe II	$z^4D_{7/2} - c^4D_{7/2}$	6319.73	4p-4s
6347.95	Si II(2)	$4s\ ^2S_{1/2} - 4p\ ^2P_{3/2}$	6348.84	···
6357.83	Fe II	$(^5D)4d\ ^4P_{5/2} - (^5D_2)4f^2[4]_{7/2}$	6358.92	?E_u
···	[Mn II]	$a^5D_0 - a^3P_1$	6359.21	···

[a]From Zethson (2001a).

[b]Taken from the "Notes" column of Zethson's tables: id? = uncertain identification; ?E_u = Fe II and Cr II transitions with an upper level $\geq$ 10 eV and the excitation mechanism is "questionable"; Not in 98 = Not present in the spectrum observed just after the 1998.0 spectroscopic event; 4p-4s = a 4p-4s transition.

Table 2. HST STIS Data

Root Name	MJD	Slit	Slit Angle (deg)[a]	Grating	Central λ (Å)	Exp Length (sec)
6307Å Observations						
o4j801120	50891.7	52x0.1	-28.	G750M	6252	9.4
o556020p0	51230.6	52x0.1	-28.	G750M	6252	8.0
o5kz010m0	51623.9	52x0.1	-28.	G750M	6252	10.0
o62r010l0	52016.8	52x0.1	+22.	G750M	6252	10.0
o6ex020l0	52294.1	52x0.1	-82.	G750M	6252	8.0
o6mo02150	52459.7	52x0.1	+69.	G750M	6252	8.0
o8gm12050	52682.9	52x0.1	-57.	G750M	6252	8.0
o8gm330r0	52776.6	52x0.1	+38.	G750M	6252	8.0
o8gm521s0	52792.0	52x0.1	+62.	G750M	6252	8.0
o8gm520h0	52812.2	52x0.1	+70.	G750M	6252	15.0
o8ma820a0	52852.0	52x0.1	+105.	G750M	6252	8.0
o8ma920z0	52904.5	52x0.1	+153.	G750M	6252	8.0
o8ma940r0	53071.3	52x0.1	-28.	G750M	6252	10.0
Fe II λ5529 Observations						
o4j8010d0	50891.5	52x0.1	-28	G750M	5734	15.0
o55602090	51230.5	52x0.1	-28	G750M	5734	15.0
o62r01090	52016.8	52x0.1	+21	G750M	5734	8.0
o6ex030b0	52183.1	52x0.1	+165	G750M	5734	15.0
o6ex02090	52294.0	52x0.1	-82	G750M	5734	6.0
o6mo020i0	52459.6	52x0.1	+69	G750M	5734	9.0
o8gm120a0	52682.9	52x0.1	-57	G750M	5734	6.0
o8gm210d0	52727.3	52x0.1	-28	G750M	5734	9.0
o8gm410d0	52764.4	52x0.1	+27	G750M	5734	9.0
o8gm320i0	52778.6	52x0.1	+38	G750M	5734	9.0
o8gm520i0	52791.8	52x0.1	+62	G750M	5734	9.0
o8gm620i0	52814.0	52x0.1	+70	G750M	5734	9.0
o8ma720h0	52825.4	52x0.1	+69	G750M	5734	9.0
o8ma820j0	52852.0	52x0.1	+105	G750M	5734	6.0
o8ma920b0	52904.4	52x0.1	+153	G750M	5734	6.0
o8ma830d0	52960.7	52x0.1	-142	G750M	5734	8.0
o8ma94080	53071.3	52x0.1	-28	G750M	5734	6.0
Spectra Used to Synthesize ACS/HRC F250W Fluxes						
o8gm12030	52682.9	52x0.1	-57.	G230MB	2836	300.0
o8gm12090	52682.9	52x0.1	-57.	G230MB	2557	800.0
o8gm120b0	52682.9	52x0.1	-57.	G430M	3680	52.0
o8gm120c0	52682.9	52x0.1	-57.	G230MB	2697	340.0
o8gm120d0	52682.9	52x0.1	-57.	G430M	3423	90.0
o8gm120h0	52683.0	52x0.1	-57.	G230MB	1995	600.0
o8gm120l0	52683.0	52x0.1	-57.	G230MB	2135	600.0
o8gm120n0	52683.0	52x0.1	-57.	G430M	3165	90.0
o8gm120r0	52683.0	52x0.1	-57.	G230MB	2416	320.0
o8gm120t0	52683.0	52x0.1	-57.	G230MB	2976	340.0
o8gm120w0	52683.0	52x0.1	-57.	G230MB	2276	600.0
o8gm33020	52776.4	52x0.1	+38.	G230MB	2135	300.0
o8gm33060	52776.4	52x0.1	+38.	G430M	3165	90.0
o8gm33090	52776.5	52x0.1	+38.	G230MB	3115	300.0
o8gm330e0	52776.5	52x0.1	+38.	G230MB	2416	320.0
o8gm330i0	52776.5	52x0.1	+38.	G230MB	2976	320.0
o8gm330n0	52776.5	52x0.1	+38.	G230MB	2276	300.0
o8gm32050	52776.6	52x0.1	+38.	G230MB	2836	300.0
o8gm320h0	52778.6	52x0.1	+38.	G230MB	2557	400.0
o8gm32l0	52778.7	52x0.1	+38.	G430M	3680	52.0
o8gm320m0	52778.7	52x0.1	+38.	G230MB	2697	340.0
o8gm320p0	52778.7	52x0.1	+38.	G430M	3423	90.0
o8gm320x0	52778.7	52x0.1	+38.	G230MB	1995	300.0
o8gm52050	52791.7	52x0.1	+62.	G230MB	2836	300.0
o8gm520h0	52791.8	52x0.1	+62.	G230MB	2557	400.0
o8gm520l0	52791.8	52x0.1	+62.	G430M	3680	52.0
o8gm520m0	52791.8	52x0.1	+62.	G230MB	2697	340.0
o8gm520p0	52791.8	52x0.1	+62.	G430M	3680	90.0
o8gm520x0	52791.8	52x0.1	+62.	G230MB	1995	300.0
o8gm52100	52791.9	52x0.1	+62.	G230MB	2135	400.0
o8gm52170	52791.9	52x0.1	+62.	G430M	3165	90.0
o8gm52180	52791.9	52x0.1	+62.	G230MB	3115	300.0
o8gm521f0	52791.9	52x0.1	+62.	G230MB	2416	320.0

Table 2—Continued

Root Name	MJD	Slit	Slit Angle (deg)[a]	Grating	Central λ (Å)	Exp Length (sec)
o8gm521j0	52791.9	52x0.1	+62.	G230MB	2976	340.0
o8gm521o0	52792.0	52x0.1	+62.	G230MB	2276	300.0
o8gm63040	52812.1	52x0.1	+70.	G230MB	2416	350.0
o8gm63080	52812.2	52x0.1	+70.	G230MB	2976	320.0
o8gm630d0	52812.2	52x0.1	+70.	G230MB	2836	300.0
o8gm62050	52813.7	52x0.1	+70.	G230MB	2836	300.0
o8gm620h0	52814.0	52x0.1	+70.	G230MB	2557	400.0
o8gm620l0	52814.1	52x0.1	+70.	G430M	3680	52.0
o8gm620m0	52814.1	52x0.1	+70.	G230MB	2697	340.0
o8gm620p0	52814.1	52x0.1	+70.	G430M	3423	90.0
o8gm620x0	52814.2	52x0.1	+70.	G230MB	1995	300.0
o8gm62100	52814.2	52x0.1	+70.	G230MB	2135	300.0
o8gm62140	52814.2	52x0.1	+70.	G430M	3165	90.0
o8ma82060	52851.9	52x0.1	+105.	G230MB	2836	300.0
o8ma820i0	52852.0	52x0.1	+105.	G230MB	2557	400.0
o8ma820m0	52852.1	52x0.1	+105.	G430M	3680	52.0
o8ma820n0	52852.1	52x0.1	+105.	G230MB	2697	340.0
o8ma820q0	52852.1	52x0.1	+105.	G430M	2697	90.0
o8ma820y0	52852.2	52x0.1	+105.	G230MB	1995	300.0
o8ma82110	52852.2	52x0.1	+105.	G230MB	2135	300.0
o8ma821a0	52852.3	52x0.1	+105.	G430M	3165	90.0
o8ma821b0	52852.3	52x0.1	+105.	G230MB	2416	320.0
o8ma821i0	52852.4	52x0.1	+105.	G230MB	2976	300.0
o8ma821m0	52852.4	52x0.1	+105.	G230MB	2276	300.0
o8ma92040	52940.3	52x0.1	+153.	G230MB	2836	300.0
o8ma920a0	52940.3	52x0.1	+153.	G230MB	2557	800.0
o8ma920c0	52940.4	52x0.1	+153.	G430M	3680	52.0
o8ma920d0	52940.4	52x0.1	+153.	G230MB	2697	340.0
o8ma920e0	52940.4	52x0.1	+153.	G430M	3423	90.0
o8ma920i0	52940.4	52x0.1	+153.	G230MB	1995	600.0
o8ma920m0	52940.4	52x0.1	+153.	G230MB	2135	600.0
o8ma920o0	52940.4	52x0.1	+153.	G430M	3350	90.0
o8ma920p0	52940.4	52x0.1	+153.	G230MB	3115	300.0
o8ma920s0	52940.5	52x0.1	+153.	G230MB	2416	600.0
o8ma920u0	52940.5	52x0.1	+153.	G230MB	2976	340.0
o8ma920x0	52940.5	52x0.1	+153.	G230MB	2276	300.0
o8ma94020	53071.3	52x0.1	-28.	G230MB	2836	320.0
o8ma94070	53071.3	52x0.1	-28.	G230MB	2557	410.0
o8ma94090	53071.3	52x0.1	-28.	G430M	2557	52.0
o8ma940a0	53071.3	52x0.1	-28.	G430M	3423	90.0
o8ma940e0	53071.3	52x0.1	-28.	G230MB	2697	323.0
o8ma940h0	53071.3	52x0.1	-28.	G430M	3165	90.0
o8ma940i0	53071.3	52x0.1	-28.	G230MB	2135	320.0
o8ma940m0	53071.3	52x0.1	-28.	G230MB	2416	450.0

[a]The slit angel is measured from north through east. All slits are peaked up on the central star.

Table 3. Measured Properties of 6307Å

MJD	Year	Telescope	Centroid (Å)	Line Flux[a] (erg cm^{-2} s^{-1})×10^{-13}	Line EW[a] (Å)
50891.7	1998.21	HST/STIS	···	2.98±1.52	-0.01±0.05[b]
51230.6	1999.14	HST/STIS	6306.88±0.19	9.77±2.66	0.19±0.05
51533.3	1999.97	VLT/UVES	6306.80±0.08	···	0.19±0.05[b]
51623.9	2000.22	HST/STIS	6306.95±0.19	8.89±1.36	0.19±0.03
52016.8	2001.29	HST/STIS	6307.32±0.19	22.62±1.63	0.39±0.03
52294.1	2002.05	HST/STIS	6306.90±0.19	14.91±1.78	0.26±0.03
52459.7	2002.51	HST/STIS	6306.75±0.19	14.92±3.20	0.24±0.05
52615.3	2002.93	VLT/UVES	6306.50±0.08	···	0.20±0.06
52620.3	2002.95	VLT/UVES	6306.69±0.08	···	0.24±0.05
52682.9	2003.12	HST/STIS	6306.75±0.19	7.62±2.56	0.14±0.05
52684.6	2003.12	VLT/UVES	6306.41±0.08	···	0.14±0.05
52776.6	2003.24	HST/STIS	···	1.79±3.56	0.03±0.06
52788.6	2003.40	VLT/UVES	···	···	0.05±0.06
52792.0	2003.42	HST/STIS	···	4.65±2.46	0.07±0.04
52794.5	2003.42	VLT/UVES	···	···	-0.01±0.04
52812.2	2003.47	HST/STIS	···	3.61±2.98	0.05±0.04
52825.5	2003.51	VLT/UVES	···	···	-0.07±0.05
52852.0	2003.58	HST/STIS	···	-1.90±2.87	-0.03±0.04
52904.5	2003.72	HST/STIS	···	-2.19±3.60	-0.03±0.04
53055.6	2004.14	VLT/UVES	···	···	0.05±0.04
53071.3	2004.18	HST/STIS	···	5.41±3.22	0.06±0.03
53413.4	2005.12	VLT/UVES	6306.99±0.08	···	0.44±0.06
53448.1	2005.21	VLT/UVES	6306.93±0.08	···	0.39±0.04

[a]Fluxes and equivalent widths are expressed relative to the continuum with values greater than zero denoting excess flux above the continuum. Only the STIS/CCD data is absolute flux calibrated.

[b]The wing of Fe II λ 6319 was brighter than normal at this time so that it interfered with the measurement of the equivalent width of the feature.